The Role of Cation−π Interactions in Biomolecular Association. Design of Peptides Favoring Interactions between Cationic and Aromatic Amino Acid Side Chains

Ekaterina V. Pletneva,*,§ Alain T. Laederach,‡ D. Bruce Fulton,† and Nenad M. Kostić*,§

Contribution from the Departments of Chemistry,§ Chemical Engineering,‡ and Biochemistry, Biophysics and Molecular Biology,† Iowa State University, Ames, Iowa 50011

Received February 14, 2001. Revised Manuscript Received April 3, 2001

Abstract: Cation−π interactions between amino acid side chains are increasingly being recognized as important structural and functional features of proteins and other biomolecules. Although these interactions have been found in static protein structures, they have not yet been detected in dynamic biomolecular systems. We determined, by ^{1}H NMR spectroscopic titrations, the energies of cation−π interactions of the amino acid derivative AcLysOMe (**1**) with AcPheOEt (**2**) and with AcTyrOEt (**3**) in aqueous and three organic solvents. The interaction energy is substantial; it ranges from −2.1 to −3.4 kcal/mol and depends only slightly on the dielectric constant of the solvent. To assess the effects of auxiliary interactions and structural preorganization on formation of cation−π interactions, we studied these interactions in the association of pentapeptides. Upon binding of the positively-charged peptide AcLysLysLysLysLysNH$_2$ (**5**) to the negatively-charged partner AcAspAspXAspAspNH$_2$ (**6**), in which X is Leu (**6a**), Tyr (**6b**), and Phe (**6c**), multiple interactions occur. Association of the two pentapeptides is dynamic. Free peptides and their complex are in fast exchange on the NMR time-scale, and 2D ^{1}H ROESY spectra of the complex of the two pentapeptides do not show intermolecular ROESY peaks. Perturbations of the chemical shifts indicated that the aromatic groups in peptides **6b** and **6c** were affected by the association with **5**. The association constants K_A for **5** with **6a** and with **6b** are nearly equal, $(4.0 \pm 0.7) \times 10^3$ and $(5.0 \pm 1.0) \times 10^3$ M^{-1}, respectively, while K_A for **5** with **6c** is larger, $(8.3 \pm 1.3) \times 10^3$ M^{-1}. Molecular-dynamics (MD) simulations of the pentapeptide pairs confirmed that their association is dynamic and showed that cation−π contacts between the two peptides are stereochemically possible. A transient complex between **5** and **6** with a prominent cation−π interaction, obtained from MD simulations, was used as a template to design cyclic peptides C$_X$ featuring persistent cation−π interactions. The cyclic peptide C$_X$ had a sequence AcLysCys(Lys)$_3$Gly(Asp)$_2$XCysAspNH$_2$, in which X is Tyr, Phe, and Leu. The first two peptides do, but the third does not, contain the aromatic residue capable of interacting with a cationic Lys residue. This covalent construct offered conformational stability over the noncovalent complexes and allowed thorough studies by 2D NMR spectroscopy. Multiple conformations of the cyclic peptides C$_{Tyr}$ and C$_{Phe}$ are in slow exchange on the NMR time-scale. In one of these conformations, cation−π interaction between Lys3 and Tyr9/Phe9 is clearly evident. Multiple NOEs between the side chains of residues 3 and 9 are observed; chemical-shift changes are consistent with the placement of the side chain of Lys3 over the aromatic ring. In contrast, the cyclic peptide C$_{Leu}$ showed no evidence for close approach of the side chains of Lys3 and Leu9. The cation−π interaction persists in both DMSO and aqueous solvents. When the disulfide bond in the cyclic peptide C$_{Phe}$ was removed, the cation−π interaction in the acyclic peptide AC$_{Phe}$ remained. To test the reliability of the pK_a criterion for the existence of cation−π interactions, we determined residue-specific pK_a values of all four Lys side chains in all three cyclic peptides C$_X$. While NOE cross-peaks and perturbations of the chemical shifts clearly show the existence of the cation−π interaction, pK_a values of Lys3 in C$_{Tyr}$ and in C$_{Phe}$ differ only marginally from those values of other lysines in these dynamic peptides. Our experimental results with dynamic peptide systems highlight the role of cation−π interactions in both intermolecular recognition at the protein−protein interface and intramolecular processes such as protein folding.

Introduction

The so-called cation−π interaction is a strong and specific interaction between a cation and the π face of an aromatic ring.[1] These interactions and their role in biomolecular structures are being vigorously studied.[2−4] In proteins, cation−π interactions can occur between the cationic side chains of lysine (Lys), arginine (Arg), or histidine (His) on one hand and the aromatic side chains of phenylalanine (Phe), tyrosine (Tyr), or tryptophan (Trp) on the other. Extensive analysis of protein structures has shown these interactions to be common within proteins.[5−7]

§ Department of Chemistry.
‡ Department of Chemical Engineering.
† Department of Biochemistry, Biophysics and Molecular Biology.

(1) Dougherty, D. A. *Science* **1996**, *271*, 163−168.
(2) Ma, J. C.; Dougherty, D. A. *Chem. Rev.* **1997**, *97*, 1303−1324.
(3) Scrutton, N. S.; Raine, A. R. C. *Biochem. J.* **1996**, *319*, 1−8.
(4) Zarić, S. D.; Popović, D. M.; Knapp, E.-W. *Chem. Eur. J.* **2000**, *6*, 3935−42.
(5) Gallivan, J. P.; Dougherty, D. A. *Proc. Natl. Acad. Sci. U.S.A.* **1999**, *96*, 9459−9464.

10.1021/ja010401u CCC: $20.00
Published on Web 06/07/2001

Furthermore, cation−π interactions have been suggested to contribute to protein stability.[5,6]

Cation−π interactions have also been implicated in protein binding to small molecules and to other proteins. Most of these cases, however, involve alkylated ammonium ligands, as in acetylcholine,[8,9] phosphocholine,[10] trimethylamines,[11,12] and dimethylamines.[13] Studies by Dougherty et al. of host−guest interactions in synthetic systems showed that protonated amines are less effective than alkylated amines in their binding to aromatic hosts, presumably because the former are more hydrophilic.[14] However, a very recent theoretical study from the same laboratory found a strong interaction between a protonated primary amine and benzene in water, more stabilizing than an analogous salt bridge.[6] This theoretical prediction suggests that cation−π interactions between common amino acid side chains may greatly contribute to protein−peptide and protein−protein recognition, but this important possibility has barely been examined experimentally. Cation−π interactions have been implicated in the binding of G protein-coupled receptors and biogenic amines,[15] the SH2 domain of the v-*src* oncogene product and tyrosine-phosphorylated peptides,[16] trypanothione reductase and spermidine-linked peptides,[17] and photosynthetic redox proteins cytochrome *f* and plastocyanin.[18] The relative importance of cation−π interactions, salt bridges, and hydrogen bonds for biomolecular association has been a subject of much interest and some debate.[19,20]

After numerous elegant studies of the energetics of cation−π interactions in synthetic systems, the energetics of these interactions in biological systems remains largely unexplored. In this paper, we report experimental energies of cation−π interactions between amino acid side chains in model systems, analyze these interactions in dynamic complexes of several pentapeptides, use this analysis to design peptides that strongly favor cation−π interaction, and show experimentally that the expected interaction indeed occurs. To our knowledge, this is the first report of the design and experimental confirmation of the cation−π interaction between two amino acid side chains in a small peptide system.

Recent molecular-dynamics (MD) simulations in this laboratory gave us the idea that the cation−π interactions may contribute to the association of the proteins cytochrome *f* and plastocyanin.[18] The cationic side chain of Lys65 in cytochrome *f* seems to interact with the aromatic side chain of the highly conserved Tyr83 in plastocyanin. In this study, we focus on the interactions of Lys with Tyr and Phe. Although our peptides somewhat resemble the interacting surfaces of cytochrome *f* and plastocyanin, we do not consider them as representative models for the associating proteins. Protein−protein association is a complex phenomenon,[21] which cannot be modeled well with amino acids and peptides.

Amino acids and peptides, however, are well suited for thorough studies of side-chain interactions that are found in proteins. Such model systems are robust, allowing experiments at various temperatures and in different solvents, and small, allowing detailed analysis of both experimental and computational results.

To estimate the energies of cation−π interactions under dynamic conditions, we determine by ^{1}H NMR spectroscopy association constants for lysine and aromatic amino acids in several solvents. To compare these interactions with the classical salt bridges and hydrogen bonds, we similarly determine association constants for several pairs of pentapeptides in which one member of the pair contains the cationic, and the other the aromatic, amino acid. We examine the interplay among the various interactions by NMR spectroscopy and molecular-dynamics simulations.

To create peptide systems that favor stable cation−π interactions, we selected from our molecular-dynamics simulations the longest-lived conformation of the complex between two pentapeptides having a prominent cation−π interaction and used this conformation as a template in the peptide design. Our approach differs from other very recent strategies for peptide design,[22−24] because it is based on the analysis of intermolecular association. In the designed peptide, we unambiguously identify an interaction between the cationic and aromatic side chains.

Experimental Procedures

Chemicals. Distilled water was demineralized to a resistivity greater than 16 MΩ·cm by a Barnsted Nanopure II apparatus and purified further with Chelex 100 resin from Bio-Rad Co. Amino acid esters AcLysOMe, AcTyrOEt, AcPheOEt, and LeuOEt and the salt CD_3-COONa were obtained from Sigma Chemical Co. The terminal amino group of LeuOEt was acetylated following a published procedure.[25] The deuteriated solvents were obtained from either Aldrich Chemical Co. or Cambridge Isotope Laboratories, Inc. All other chemicals were obtained from Aldrich Chemical Co. The peptides were synthesized by a standard solid-state method, and their purity was checked by HPLC separation and MALDI mass spectroscopy.

When needed, peptides were purified by the reverse-phase HPLC with a Hewlett-Packard 1100 system containing a Vydac C-18 column 218TP101522. The detector was set at 215 nm. The eluting solvents were 0.1% trifluoroacetic acid (TFA) in H_2O, designated A, and 0.08% TFA in acetonitrile, designated B. The percentage of the solvent B in the eluent was kept at 0% for 5 min after the injection of the sample, and then increased gradually to 45% over a 35 min period. The flow rate was 10 mL/min.

The disulfide bond between two cysteine residues was formed by oxidation with $K_3[Fe(CN)_6]$.[26] The resulting cyclic peptides were purified by HPLC as described above. In later experiments, to cleave

(6) Gallivan, J. P.; Dougherty, D. A. *J. Am. Chem. Soc.* **2000**, *122*, 870−874.
(7) Minoux, H.; Chipot, C. *J. Am. Chem. Soc.* **1999**, *121*, 10366−72.
(8) Sussman, J. L.; Harel, M.; Frolow, F.; Oefner, C.; Goldman, A.; Toker, L.; Silman, I. *Science* **1991**, *253*, 872−879.
(9) Zhong, W.; Gallivan, J. P.; Zhang, Y.; Li, L.; Lester, H. A.; Dougherty, D. A. *Proc. Natl. Acad. Sci. U.S.A.* **1998**, *95*, 12088−12093.
(10) Satow, Y.; Cohen, G. H.; Padlan, E. A.; Davis, D. R. *J. Mol. Biol.* **1986**, *190*, 593−604.
(11) Bellamy, H. D.; Lim, L. W.; Mathews, F. S.; Dunham, W. R. *J. Biol. Chem.* **1989**, *264*, 11887−11892.
(12) Raine, A. R. C.; Yang, C.-C.; Packman, L. C.; White, S. A.; Mathews, F. S.; Scrutton, N. S. *Protein Sci.* **1995**, *4*, 2625−2628.
(13) Yang, C.-C.; Packman, L. C.; Scrutton, N. S. *Eur. J. Biochem.* **1995**, *232*, 264−271.
(14) Kearney, P. C.; Mizoue, L. S.; Kumpf, R. A.; Forman, J. E.; McCurdy, A.; Dougherty, D. A. *J. Am. Chem. Soc.* **1993**, *115*, 9907−19.
(15) Nordvall, G.; Hacksell, U. *J. Med. Chem.* **1993**, *36*, 967−976.
(16) Waksman, G.; Kominos, D.; Robertson, S. C.; Pant, N.; Baltimore, D.; Birge, R.; Cowburn, D.; Hanafusa, H.; Mayer, B. J.; Overduin, M.; Resh, M. D.; Rios, C. B.; Silverman, L.; Kuriyan, J. *Nature (London)* **1992**, *358*, 646−653.
(17) Bailey, S.; Smith, K.; Fairlamb, A. H.; Hunter, W. N. *Eur. J. Biochem.* **1993**, *213*, 67−75.
(18) Ullmann, G. M.; Knapp, E.-W.; Kostić, N. M. *J. Am. Chem. Soc.* **1997**, *119*, 42−52.
(19) Befort, K.; Tabbara, L.; Kling, D.; Maigret, B.; Kieffer, B. L. *J. Biol. Chem.* **1996**, *271*, 10161−10168.
(20) Wess, J.; Maggio, R.; Palmer, J. R.; Vogel, Z. *J. Biol. Chem.* **1992**, *267*, 19313−19319.
(21) Stites, W. E. *Chem. Rev.* **1997**, *97*, 1233−1250.
(22) Yahalom, D.; Rahimipour, S.; Koch, Y.; Ben-Aroya, N.; Fridkin, M. *Med. Chem.* **2000**, *43*, 2831−6.
(23) Hruby, V. J.; Balse, P. M. *Curr. Med. Chem.* **2000**, *7*, 945−70.
(24) Carulla, N.; Woodward, C.; Barany, G. *Biochemistry* **2000**, *39*, 7927−37.
(25) Kondo, M.; Miyazaki, K.; Kodama, H.; Horimoto, H. *Bull. Chem. Soc. Jpn.* **1985**, *58*, 1171−3.
(26) Walker, J. M., Ed. *The Protein Protocols Handbook*; Humana Press: Totowa, NJ, 1996.

the disulfide bridge in the cyclic peptide C_{Phe} and maintain the cysteine residues in the reduced (sulfhydryl) form, approximately a 4-fold molar excess of dithiothreitol was added to the aqueous solution of the peptide at pH 7.6.

Proton NMR Spectroscopy. The ^{1}H NMR spectra were recorded with a Bruker DRX500 spectrometer and referenced to the methyl signal of sodium 2,2-dimethyl-2-silapentane-5-sulfonate (DSS) in aqueous solutions, and to the methyl signal of tetramethylsilane (TMS) in all other solvents. The temperature controller was calibrated with a methanol standard.[27]

One-dimensional ^{1}H spectra were acquired with an FID of 16 000 points, 8 to 64 averaged transients, and a spectral width of 5000 Hz. The solvent signal in the one-dimensional spectra was suppressed by presaturation during the relaxation delay.

For pentapeptides, two-dimensional ^{1}H ROESY (rotating-frame Overhauser enhancement spectroscopy) spectra[28] were acquired in aqueous solution. The ROESY experiment was chosen over NOESY[29] because the magnitude of the rotating-frame cross-relaxation is favorable for molecules of this size. For the cyclic peptides C_X (those containing a disulfide bond) and their reduced counterparts (containing two free cysteines), two-dimensional ^{1}H NOESY[30] and TOCSY[31] spectra were recorded in DMSO-d_6 or aqueous buffer or both solvents. All two-dimensional data sets consisted of 400 × 1024 complex points; each FID was an average of 16 to 64 transients. The States-TPPI method was used for quadrature detection in the indirect dimension.[32] A mixing time of 500 ms was used in NOESY and ROESY experiments, and 80 ms in TOCSY experiments. To assess the contribution of spin-diffusion to the spectra, a NOESY spectrum of the peptide C_{Tyr} in DMSO-d_6 was also acquired with a mixing time of 100 ms. The spin-lock field strength during mixing was 2.5 kHz in ROESY experiments and 6.4 kHz in TOCSY experiments. DIPSI-2 was used for isotropic mixing in TOCSY experiments.[33] For aqueous samples, WATERGATE[34] was incorporated into the pulse sequences, to suppress the solvent signal.[35−37]

All NMR data were processed with Bruker Xwinnmr 2.5 and 1D Win-NMR 6.0 software. Two-dimensional NMR data were processed also with NMRPipe[38] and were analyzed with the NMRView software.[39]

Studies of Association. All the experiments were done at 25 °C. Aliquots of a solution of the titrant, M_2, were incrementally added to an NMR tube containing a solution of the compound titrated, M_1. In a typical experiment, the initial concentration of M_1 was 1.0−2.0 mM and known precisely. The final ratio of concentrations $[M_2]/[M_1]$ reflected the extent of association and varied from 2.5 to 60. The component M_2 usually was a solution of the partner containing the cationic side chain. In control experiments, done in a mixture of CD_3-OD and $CDCl_3$, the concentration of AcLysOMe was held constant, and AcPheOEt or AcTyrOEt was used as the titrant. The two titration protocols, with different partners as M_2, yielded similar association constants, K_A, as Table S1 in the Supporting Information shows.

Peaks were picked and chemical shifts determined manually, taking into account the effects of overlap on the peak shape. The K_A values were determined from a global fitting to eq 1 of titration curves for all monitored peaks.[40] In eq 1, $\Delta\delta$ is the change in chemical shift, and $\Delta\delta_\infty$ is this change when the ratio $[M_2]/[M_1]$ approaches infinity. The free energies of complexation, $\Delta G°$, were calculated from the K_A values according to eq 2.

$$\Delta\delta = \frac{1}{2}\Delta\delta_\infty\{[M_2] + [M_1] + K_A^{-1} - \sqrt{([M_2] + [M_1] + K_A^{-1})^2 - 4[M_2][M_1]}\} \quad (1)$$

$$\Delta G° = -RT \ln K_A \quad (2)$$

The aqueous solvent was a sodium acetate-d_3 buffer at the ionic strength of 10 mM and pH 5.5 containing 10% (v/v) D_2O. The pH values were measured with a Fisher Accumet 805 MP pH meter equipped with an Aldrich combination microelectrode, standardized in H_2O solutions. The concentrations of all the solutions involved were determined by NMR integration, using DSS as a primary standard. When needed, the pH of the stock solutions was adjusted to 5.5 by the addition of NaOH or CD_3COOH solutions. Since the buffer consisted of a monoprotic acid and its conjugate base, such adjustment did not alter the ionic strength.[41] To avoid any interference from the standard compound in the titration experiments, a solution of DSS in the same buffer was placed in a Wilmad coaxial insert in the NMR tube.

Concentrations of nonaqueous solutions were determined by weighing the solute. In the experiments done in DMSO-d_6 and in a mixture of CD_3OD and $CDCl_3$, residual water affected the chemical shifts of several resonances. To keep the solvent conditions as nearly constant as possible, 1% (v/v) of water was added to these solvents, and the concentration of M_1 was carefully held constant. The dielectric constant (ϵ) of the mixed-solvent systems was interpolated from tables.[42]

Binding curves were analyzed with SigmaPlot v. 5.0, from SPSS Inc. Each titration was done at least twice. The error margins for all results include two standard deviations and correspond to a confidence limit greater than 95%.

Molecular-Dynamics Simulations. To sample the conformational space of the pentapeptide pairs (complexes), a total of six 200-ps trajectories were computed using the original Verlet algorithm implemented in version 27b2 of CHARMM.[43] An integration step of 1 fs was used, and every 100 steps structures were stored, for further analysis. Velocities were scaled every 1 ps, to a temperature of 300 K. All simulations were done on a Dell Precision 410 workstation running Linux version 2.2.5-15.

Initial random coordinates of each pentapeptide complex were generated in three steps. The extended conformation of each of the two associating pentapeptides was minimized in vacuo over 1000 time steps using the steepest-descent algorithm in CHARMM.[43] The centers of mass of the two minimized structures were overlaid, and then translated ±6 Å along six arbitrarily defined orthogonal vectors. The complexes were minimized again by the same procedure. The resulting coordinates were superimposed onto a 33.6-Å cube containing 1269 preequilibrated TIP3-type water molecules. All water molecules approaching within 3.0 Å of any of the peptide atoms were deleted.

Periodic boundary conditions were applied with cubic geometry. Particle Mesh Ewald (PMEwald) summation was used for the evaluation of the electrostatic interactions.[44] A total of 36 grid points were used, with an effective grid spacing of 0.93 Å. The Gaussian width KAPPA parameter was set to 0.34 with an ORDER of 6. Prior to sampling, 200 steps of minimization, 15 ps of heating (from 0 to 300 K), and 15 ps of equilibration were computed.

(27) Van Geet, A. L. *Anal. Chem.* **1970**, *42*, 679−680.
(28) Bothner-By, A. A.; Stephens, R. L.; Lee, J. M.; Warren, C. D.; Jeanloz; R. W. *J. Am. Chem. Soc.* **1984**, *106*, 811−813.
(29) Jeener, J.; Meier, B. H.; Bachman, P.; Ernst, R. R. *J. Chem. Phys.* **1979**, *71*, 4546−53.
(30) Macura, S.; Huang, Y.; Suter, D.; Ernst, R. R. *J. Magn. Reson.* **1981**, *43*, 259−281.
(31) Braunschweiler, L.; Ernst, R. R. *J. Magn. Reson.* **1983**, *53*, 521−528.
(32) Marion, D.; Ikura, M.; Tschudin, R.; Bax, A. *J. Magn. Reson.* **1989**, *85*, 393−399.
(33) Shaka, A. J.; Lee, C. J.; Pines, A. *J. Magn. Reson.* **1988**, *77*, 274−293.
(34) Piotto, M.; Saudek, V.; Sklenar, V. *J. Biomol. NMR* **1992**, *2*, 661−665.
(35) Lippens, G.; Dhalluin, C.; Wieruszeski, J.-M. *J. Biomol. NMR* **1995**, *5*, 327−331.
(36) Fulton, D. B.; Hrabal, R.; Ni, F. *J. Biomol. NMR* **1996**, *8*, 213−218.
(37) Fulton, D. B.; Ni, F. *J. Magn. Reson.* **1997**, *129*, 93−97.
(38) Delaglio, F.; Grzesiek, S.; Vuister, G. W.; Zhu, G.; Pfeifer, J.; Bax, A. *J. Biomol. NMR* **1995**, *6*, 277−293.
(39) Johnson, B. A.; Blevins, R. A. *J. Biomol. NMR* **1994**, *4*, 603−614.
(40) Pletneva, E. V.; Fulton, D. B.; Kohzuma, T.; Kostić, N. M. *J. Am. Chem. Soc.* **2000**, *122*, 1034−1046.
(41) Perrin, D.; Dempsey, B. *Buffers for pH and Metal Ion Control*; Halsted Press: New York, NY, 1979.
(42) Landolt, H. *Numerical data and functional relationships in science and technology*; Madelung, O., Ed.; Springer-Verlag: Berlin, Germany, 1991; Vol. 6.
(43) Brooks, B. R.; Bruccoleri, R. E.; Olafson, B. D.; States, D. J.; Swaminathan, S.; Karplus, M. *J. Comput. Chem.* **1983**, *4*, 187−217.
(44) Feller, S. E.; Pastor, R. W.; Rojnuckarin, A.; Bogusz, S.; Brooks, B. R. *J. Phys. Chem.* **1996**, *100*, 17011−20.

For all the stored structures, distances from Lys(N^{ϵ}) to Asp(C^{γ}) were computed. The distances from Lys(N^{ϵ}) to aromatic C atoms in Tyr or Phe were averaged and used as a rough measure of the approach of the ammonium cation to the π system. The side chains were considered interacting if the above-mentioned distances fell below 8.0 Å, a distance that includes the radii of the ions and the thickness of the water layer between them.[18]

In the design of a cyclic peptide that favors cation−π interactions, all the stored structures of the pentapeptide complexes were considered as potential templates. The principle of our design strategy was to link the backbone of two associating pentapeptides by connecting the *N*-terminus of one peptide with the *C*-terminus of the other. To make the peptide cyclic, one salt bridge was replaced with a pair of cysteine residues forming a disulfide bond.

Several criteria were used to select templates from the stored structures. Complexes in which the π system closely approached at least one Lys side chain were extracted. In deciding how to link the *N*-terminus of one pentapeptide with the *C*-terminus of the other without significantly altering the conformations of the peptide backbones, intermolecular distances between *N*-terminus and *C*-terminus were measured in potential template structures. If this intermolecular distance was less than the intermolecular distance between the two *N*-termini, the template was accepted.

This last criterion also decided which *N* and *C* termini to link with a glycine residue. Once a template was accepted, the protecting groups were removed from the closest *N*-terminus and *C*-terminus of the opposing pentapeptides. A glycine residue was inserted between them, and an amide bond was made to both *N*-terminus and *C*-terminus chosen for connection. Attempts to introduce two glycine residues as a linker between the termini yielded unsatisfactory results; one glycine residue proved to be a better linker. One of the salt-bridged Lys-Asp pairs was then replaced with a disulfide-bonded Cys pair. Any water molecules located within 3 Å of the added atoms were removed.

Each cyclic peptide was then minimized in 10 000 steps, using the steepest-descent algorithm. The atomic distances between the interacting side chains were harmonically constrained, with a force constant of 100 kcal/mol Å, to a value equal to that measured in the template. The distance restraints were then removed, and 5 ps of heating (0 to 300 K) was followed by 10 ps of Verlet MD simulation. Every 1000 integration steps, velocities were scaled to 300 K. For cyclic peptides in which one or more Lys side chains kept interacting with the aromatic system after the 15 ps, longer MD trajectories were computed. The peptide with the longest-lived lysine-aromatic interaction was chosen for the experimental work: synthesis, purification, and NMR spectroscopic study. The symbol C_X represents a designed cyclic peptide containing the residue X (Leu, Tyr, or Phe) in position 9.

Structure Calculations and NMR Constraints. The structures of the cyclic peptides in solution were determined using CNS version 1.0.[45] The NOE constraints were classified as strong (≤2.8 Å), medium (≤3.4 Å), or weak (≤5.0 Å) on the basis of the relative intensities of the NOESY cross-peaks. For the cyclic peptides C_{Tyr} and C_{Phe}, two sets of chemical shifts were observed for each of the residues 3, 9, and 10; thus also the primed set 3′, 9′, and 10′. There were several NOE cross-peaks between residues 9′ and 10′, suggesting that these belong to the same peptide conformation. The observed NOE peaks were divided into three distinct groups: C_X* (containing residues 3, 9, and 10), $C_X^{3'}$ (containing residues 3′, 9, and 10), and $C_X^{9'10'}$ (containing residues 3, 9′, and 10′). All in all, the NMR spectra yielded three different sets of distance constraints. Each set contained 120−150 NOE-based distance constraints. Starting from an extended peptide strand, 100 runs of dynamical annealing were performed.[46,47] The coordinates of the 10 lowest-energy structures were averaged and minimized. These structures were superimposed with MolMol software.[48] If one of the ten calculated structures significantly deviated from the others, it was omitted from the calculation of the average structure.

Chart 1

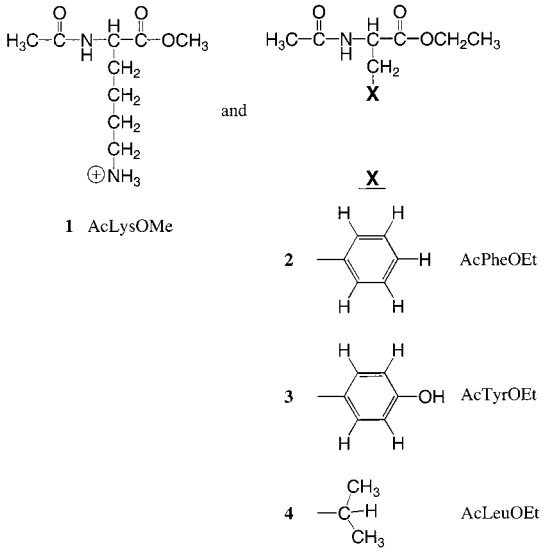

Determination of Acid Dissociation Constants of Lysine Side Chains. For pK_a determination, 1.0−2.0 mM solutions of each cyclic peptide in a sodium acetate-d_3 buffer at pH 5.5 containing 10% (v/v) D_2O were prepared. These studies were done in aqueous solution and at 25 °C. Under these conditions, multiple conformations of the cyclic peptide C_X are in fast exchange on the NMR time-scale. The pH of the sample was adjusted with a solution of NaOH in the same buffer. A small amount of DSS (200 μM) was added for a chemical-shift reference. The measured pH values were used.[49] Two-dimensional ^{1}H TOCSY spectra were recorded at different pH values; 16−32 data points were collected in the *t*2 dimension, and 400 increments were used in the *t*1 dimension. In these spectra, the $C^{\alpha}H-C^{\epsilon}H$ cross-peaks for Lys residues were monitored to obtain the chemical shifts of the $C^{\epsilon}H$ protons for each of the four Lys residues in the peptides C_X.[49]

Twelve titration curves were obtained, one for each of the four Lys residues in each of the three cyclic peptides C_X, in which X is Leu, Tyr, or Phe. The acid-dissociation constant, K_a, was determined from fitting of the titration curve to eq 3,[49] in which δ_{HA} and δ_A are the $C^{\epsilon}H$ chemical shifts when the adjacent amino group is in its acidic (protonated) and basic (deprotonated) forms, respectively; and a_{H^+} is the activity of the hydrogen ion.

$$\delta_{obs} = \frac{a_{H^+}\delta_{HA} + K_a\delta_A}{a_{H^+} + K_a} \qquad (3)$$

Results and Discussion

Studies of Cation−π Interactions between Amino Acid Side Chains in Various Solvents. For studies of the interactions between the cationic side chain of Lys and aromatic side chains of Tyr and Phe, we chose the *N*-acetylated amino acid esters designated **1**−**3** and shown in Chart 1. In these compounds terminal amino and carboxylic groups are blocked, to suppress classical electrostatic interactions and hydrogen bonds and to favor cation−π interactions. We study association of the cationic compound **1** with aromatic compounds **2** and **3** by ^{1}H NMR spectroscopy. Multiple signals, corresponding to protons in both partners, were affected by the titrations. The complexation-induced perturbations of the chemical shifts were small (0.01 ppm or less), but reproducible (see Figure S1 in the Supporting

(45) Brunger, A. T.; Adams, P. D.; Clore, G. M.; DeLano, W. L.; Gros, P.; Grosse-Kunstleve, R. W.; Jiang, J. S.; Kuszewski, J.; Nilges, M.; Pannu, N. S.; Read, R. J.; Rice, L. M.; Simonson, T.; Warren, G. L. *Acta Crystallogr. D Biol. Crystallogr.* **1998**, *54*, 905−21.

(46) Kuszewski, J.; Gronenborn, A. M.; Clore, G. M. *J. Magn. Reson., Ser. B* **1996**, *112*, 79−81.

(47) Nilges, M.; Gronenborn, A. M.; Brunger, A. T.; Clore, G. M. *Protein Eng.* **1988**, *2*, 27−38.

(48) Koradi, R.; Billeter, M.; Wüthrich, K. *J. Mol. Graphics* **1996**, *14*, 51−55.

(49) Rabenstein, D. L.; Hari, S. P.; Kaerner, A. *Anal. Chem.* **1997**, *69*, 4310−4316.

Table 1. Association Constants (K_A),[a,b] and Free Energies of Complexation ($\Delta G°$)[b] Calculated from Them, for the Binding of AcLysOMe (**1**) to AcPheOEt (**2**) and to AcTyrOEt (**3**) in Various Solvents at 25 °C

	AcPheOEt		AcTyrOEt	
solvent system	K_A, M^{-1}	$-\Delta G°$, kcal/mol	K_A, M^{-1}	$-\Delta G°$, kcal/mol
$CDCl_3/CD_3OD+H_2O$ (4:1+1%v/v)	300 ± 20	3.4 ± 0.1	130 ± 20	2.9 ± 0.1
DMSO+1%v/v H_2O	150 ± 30	3.0 ± 0.2	40 ± 4	2.2 ± 0.1
CD_3CN/H_2O mixture (2:3 w/w)	260 ± 60	3.3 ± 0.2	70 ± 10	2.5 ± 0.1
NaOAc buffer pH 5.5 (aq)+10%v/v D_2O	59 ± 7	2.4 ± 0.1	35 ± 11	2.1 ± 0.2

[a] The value of K_A was obtained from the fitting of the average perturbations of chemical shifts, determined in at least two independent titrations. [b] The error margins include two standard deviations and correspond to the confidence limit greater than 95%

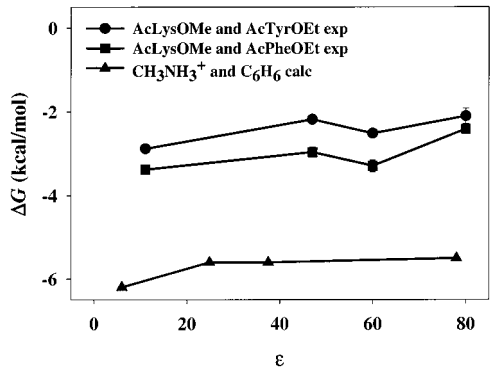

Figure 1. Interaction energies for possible cation−π pairs plotted against the dielectric constant of the solvent. The interaction energies for the methylammonium−benzene pair, calculated at the SM5.42R/HF/6-31+G* level, were taken from ref 6. As discussed in ref 6, the calculations overestimate the interaction energy; the corrected value for this cation−π interaction in water is approximately −3.6 kcal/mol.

Information). Peak splitting was never observed, evidence that the exchange between the complex and the free amino acid derivatives is fast on the NMR time-scale. Association constants, K_A, and corresponding free energies of complexation, $\Delta G°$, are given in Table 1.

Binding was studied in four solvents. Because the lysine $N^{\epsilon}H_3^+$ group rapidly exchanges H^+ ions with water, it was impossible to detect this signal directly in water and in acetonitrile/water mixture. In the other two solvent systems, the addition of aromatic compounds **2** or **3** to a solution of **1** induced an upfield movement of the $N^{\epsilon}H_3^+$ signal; this behavior is consistent with placement of an ammonium group above an aromatic ring. The addition of cationic compound **1** to solutions of **2** and **3** caused the signals of aromatic protons to move upfield in water, and downfield in the other solvents. The complexation-induced perturbations of chemical shifts may depend on the solvent and generally are difficult to predict.[50] The cation−π interaction is known to cause downfield movements of aromatic signals in some systems.[51,52] For example, such movements were observed upon binding of metal cations to calix[4]arenes in a chloroform/methanol mixture;[51] in our system, too, the signals move downfield in this solvent. In the control experiments with AcLeuOEt (designated **4**), the chemical shifts of **4** were unaffected by the addition of AcLysOMe. Taken together, our findings are consistent with cation−π interactions between the cationic side chain of Lys and the aromatic side chains of Tyr and Phe.

As Table 1 shows, the interactions take place in all four solvents studied. In Figure 1, the interaction energies are plotted against the dielectric constant of the solvent. In the range studied, the strength of the interactions depends only weakly on the dielectric constant. Our experimental results confirm a very recent theoretical prediction by Gallivan and Dougherty.[6]

The hydroxyl group in the aromatic ring of AcTyrOEt can act as a hydrogen bond acceptor. Indeed, we detect characteristic downfield movement of the OH signal of Tyr upon addition of AcLysOMe. Moreover, the two aromatic protons adjacent to the OH group moved downfield more than the other two aromatic protons did (see Figure S2 in the Supporting Information). Upfield movement of the lysine $N^{\epsilon}H_3^+$ signal, however, is a strong indication of a possible cation−π interaction. We conclude that both cation−π and hydrogen bonding interactions may contribute to the association of the two amino acid derivatives. These interactions can both be important, and they likely work in concert.[5] In addition, a number of hydrophobic interactions are possible between the methylene groups of Lys and the aromatic ring of Tyr and Phe.[53] Therefore, the results in Table 1 reflect not only the cation−π interaction, but also other interactions between a cationic side chain and an aromatic side chain.

Table 1 shows that Lys binds more strongly to Phe than to Tyr in all the solvents used. These results contradict the proposal that the cation−π binding ability of the Tyr side chain should be higher because the oxygen atom of Tyr provides an additional site of highly negative electrostatic potential.[1] We suggest that in all the studied solvents Tyr is better solvated than Phe, and that a very unfavorable process of desolvation lowers the overall affinity of Tyr for the Lys side chain. Although Tyr may have a higher intrinsic cation−π binding ability than Phe, solvation energy in water is about 5 kcal/mol more negative for Tyr than for Phe.[54,55] Since cation−π parters are rarely found completely buried within proteins,[6] their interaction may well be modulated by solvation effects.

Our experimental $\Delta G°$ values, −2.1 to −2.4 kcal/mol, for possible cation−π interactions of amino acid side chains in water are consistent with those reported for synthetic host−guest systems and biological systems. Our values fall well in the range −0.5 to −2.6 kcal/mol determined experimentally,[14,56−59] and are close to the values −3.2 and −3.6 kcal/mol predicted theoretically.[6,60] Our experimental findings further suggest that cation−aromatic interactions between amino acid side chains can be rather strong, similar to salt bridges and hydrogen bonds.

Studies of Pentapeptide Association in Aqueous Media.

(50) Günther, H. *NMR Spectroscopy: Basic Principles, Concepts, and Applications in Chemistry*; Wiley: New York, 1995.
(51) Ikeda, A.; Shinkai, S. *J. Am. Chem. Soc.* **1994**, *116*, 3102−3110.
(52) Kubik, S. *J. Am. Chem. Soc.* **1999**, *121*, 5846−5855.
(53) Karlin, S.; Zuker, M.; Brocchieri, L. *J. Mol. Biol.* **1994**, *239*, 227−48.
(54) Privalov, P. L.; Makhatadze, G. I. *J. Mol. Biol.* **1993**, *232*, 660−679.
(55) Smith, B. J. *J. Comput. Chem.* **1999**, *20*, 428−442.
(56) Schneider, H.-J.; Schiestel, T.; Zimmermann, P. *J. Am. Chem. Soc.* **1992**, *114*, 7698−703.
(57) Schneider, H.-J. *Chem. Soc. Rev.* **1994**, 227−34.
(58) Loewenthal, R.; Sancho, J.; Fersht, A. R. *J. Mol. Biol.* **1992**, *224*, 759−770.
(59) Ting, A. Y.; Shin, I.; Lucero, C.; Schultz, P. G. *J. Am. Chem. Soc.* **1998**, *120*, 7135−7136.
(60) Chipot, C.; Maigret, B.; Pearlman, D. A.; Kollman, P. A. *J. Am. Chem. Soc.* **1996**, *118*, 2998−3005.

To test the effects of the auxiliary interactions and structural preorganization on the cation−π interactions between amino acid side chains, we studied peptide association, an intermolecular process. An intramolecular system might at first appear more suitable for construction of a desired interaction. Indeed, statistical analysis of cation−π interactions in proteins revealed that these interactions are most common between neighboring residues in the sequence.[5] When, however, interacting amino acid residues belong to the same peptide chain, factors besides cation−π interactions may be responsible for the conformation that brings the residues into contact. Because even short peptides in solution may exhibit significant secondary structure,[61,62] conformation of a single chain cannot reliably be attributed to a particular interaction within the chain.

In this study of the cation−π interactions, we place a cationic group and an aromatic group onto different peptide strands. In our method, the proximity of the side chains belonging to different peptides is a strong indication that these side chains have a special affinity for each other. Moreover, in a study of interactions *between* peptides rather than *within* a peptide, binding affinities of various peptide pairs can be determined and analyzed. Because peptide recognition is an intricate phenomenon,[63−65] a rational design of selective interactions between small peptides is difficult. Peptide association is far less specific than protein association, but the study of peptides also has its advantages. Their intrinsic flexibility makes their association a dynamic process, interesting in its own right, and is related to some protein−protein interactions.[66]

We study the binding of two oppositely-charged pentapeptides, designated **5** and **6** in Chart 2. Their terminal amino and carboxylic groups are blocked, to minimize electrostatic attractions among the molecules of the same kind and thus suppress peptide self-association. The electrostatic attraction between oppositely-charged ionic groups brings the two peptides together and may favor a cation−π interaction between the ammonium cation in the one peptide and the aromatic ring in the other. Because of the relevance of these interactions to biomolecular association, we studied peptide association in aqueous solution. Under these conditions, salt bridges and possible cation−π interactions must compete with the favorable solvation of ionic side chains and other polar groups. To overcome the desolvation penalty and ensure binding, we gave the peptides high opposite charges.

The addition of pentalysine, **5**, to solutions of pentapeptides **6** perturbed chemical shifts of many signals, corresponding to protons in both partners. These complexation-induced perturbations were reproducible and larger (up to 0.05 ppm) than those found with single amino acids (see Figure S3 in the Supporting Information). Again, absence of peak splitting rules out slow exchange between the complex and free peptides. Two-dimensional ^{1}H NMR ROESY spectra of the pairs of associating pentapeptides did not contain any intermolecular ROESY peaks. Association constants, K_A, and corresponding free energies of complexation, $\Delta G°$, are given in Table 2.

Chart 2

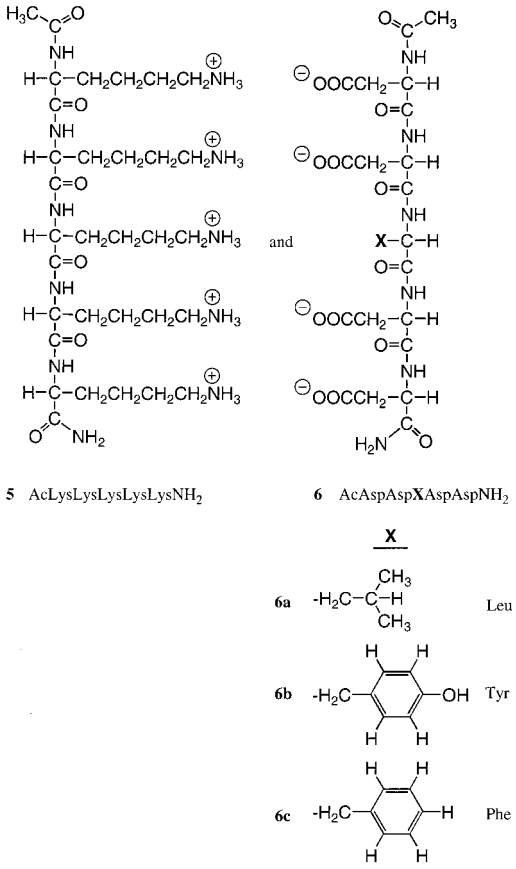

Table 2. Association Constants (K_A), and Free Energies of Complexation ($\Delta G°$) Calculated from Them, for the Binding of $AcLysLysLysLysLysNH_2$ (**5**) to $AcAspAspXAspAspNH_2$ (**6**) at 25 °C[a]

residue X	pentapeptide	$K_A \times 10^{-3}$, M^{-1} [b,c]	$-\Delta G°$, kcal/mol[c]
Leu	**6a**	4.0 ± 0.7	4.9 ± 0.1
Tyr	**6b**	5.0 ± 1.0	5.0 ± 0.1
Phe	**6c**	8.3 ± 1.3	5.3 ± 0.1

[a] All titrations were done in a sodium acetate buffer of ionic strength 10 mM and pH 5.5 containing 10% (v/v) D_2O. [b] The value of K_A was obtained from the fitting of the average perturbations of chemical shifts, determined in at least two independent titrations. [c] The error margins include two standard deviations and correspond to the confidence limit greater than 95%.

In aqueous solution, the NMR signals corresponding to aromatic protons in both Tyr-containing and Phe-containing pentapeptides, **6b** and **6c**, moved upfield upon addition of pentalysine, **5**. In the control experiments done in DMSO solution, those signals moved downfield. In both solvents, the aromatic protons in pentapeptides move in the same direction upon complexation with the cationic partner as the aromatic protons in our studies of single amino acids. The Leu signals in the pentapeptide **6a** did not move upon addition of **5**. These findings consistently indicate that the aromatic groups in peptides **6b** and **6c** are affected by the complexation, and the aliphatic group in the peptide **6a** is not.

The association constants in Table 2 are relatively large. Evidently, the high opposite charges of the two peptides cause strong attractions between their side chains, even in aqueous solution. The dependence of K_A on the identity of the residue X is subtle but significant. Association constants for **6a** and **6b** are nearly equal, considering the error margins. However, the two-dimensional ^{1}H NMR ROESY spectra suggest that the

(61) Wright, P. E.; Dyson, H. J.; Lerner, R. A. *Biochemistry* **1988**, *27*, 7167−7175.
(62) Gierasch, L. M.; Deber, C. M.; Madison, V.; Niu, C. H.; Blout, E. R. *Biochemistry* **1981**, *20*, 4730−8.
(63) Boyce, R.; Li, G.; Nestler, H. P.; Suenaga, T.; Still, C. *J. Am. Chem. Soc.* **1994**, *116*, 7955−6.
(64) Sasaki, S.; Takagi, M.; Tanaka, Y.; Maeda, M. *Tetrahedron Lett.* **1996**, *37*, 85−88.
(65) Hossain, M. A.; Schneider, H.-J. *J. Am. Chem. Soc.* **1998**, *120*, 11208−9.
(66) Bendall, D. S. In *Protein Electron Transfer*; Bendall, D. S., Ed.; BIOS Scientific Publishers Ltd: Oxford, UK, 1996; pp 43−68.

pentapeptide **6a** differs in conformation from **6b** and **6c**, which are alike (see Figure S4 in the Supporting Information). While the Leu-containing pentapeptide, **6a**, is predominantly random-coiled, the two other pentapeptides, **6b** and **6c**, are somewhat structured, as evidenced by the cross-peaks of Tyr3/Phe3 with both of its neighbors, Asp2 and Asp4. Consistent with these ROESY peaks, the molecular-dynamics simulations described below show a general preference for a "horse-shoe" conformation of the backbones in **6b** and **6c**. The different structure of the peptide **6a** prevents direct comparison of its binding affinity with those of **6b** and **6c**, whereas the last two can be compared. The moderate increase in the association constant from **6b** to **6c** suggests that Phe provides more favorable interaction than Tyr does. As in the case of interacting single amino acids (Table 1), we attribute the higher affinity of **6c** to a lower desolvation penalty of the Phe side chain in water. Although the differences in the association constants are small, these binding studies indicate that the peptides **5** and **6** do bind and that the aromatic residues in **6** may contribute to the increase in the binding affinity.

Although chemical-shift changes and the differences in association constants strongly suggest that aromatic residues play a role in the association, we do not rely on ^{1}H NMR spectroscopic titrations alone to decide whether cation$-\pi$ interactions between amino acid side chains are formed in the complex structures. The possibility of conventional salt bridges, hydrogen bonds, and hydrophobic interactions, as well as cation$-\pi$ interactions, and the dynamic nature of small peptides association complicate the analysis of binding experiments. To explore further the association of the two pentapeptides, we simulated their complexes by molecular dynamics.

Molecular-Dynamics Simulations of Pentapeptide Association. In performing molecular-dynamics (MD) simulations of the pentapeptide complexes (pairs) that **5** makes with **6a**, **6b**, and **6c**, we sought to answer the following two questions. Are there preferred conformations of the pentapeptide complexes? Can the cationic side chain of Lys approach the aromatic ring of Tyr or Phe without steric hindrance from the other side chains? Our goal was not to search exhaustively the conformational space and reproduce the measured association constants.[67] Rather, we wanted to generate a representative set of structures, so that we can understand the contribution of the cationic and aromatic side chains to the peptide association.

The cation$-\pi$ complex involves various intermolecular forces, such as charge-quadrupole, charge-dipole, charge-induced dipole, and hydrophobic interactions; charge transfer; and dispersion forces.[1] Although electrostatic interactions play a prominent, and sometimes dominant, role in the cation$-\pi$ interactions,[2] polarization of the π system by the cation is also important.[68] The empirical force field in CHARMm does not take into account the polarizability of the aromatic system. A 10$-$12 term can be added to empirical force fields, to account for the effect of the polarization of the π system.[60] We considered such a correction unnecessary for the system under study. The maximum attractive contribution of the correction is 0.7 kcal/mol at 3.5 Å. As our experiments showed, association of the highly-charged peptides **5** and **6** is primarily governed by Coulombic attraction. Therefore, a small correction by the 10$-$12 term would only marginally alter the potential-energy surface. The CHARMm force field, already optimized to reproduce known peptide conformers,[69] sufficed for our purposes.

Because solvation effects are critically important to interactions of the two highly charged peptides, we used an explicit solvent system with periodic boundary conditions. Our simulation time was relatively short. To ensure a more complete sampling of the conformational space, we ran six simulations in parallel, with different initial conformations.

From the NMR results, we knew that the association of the two pentapeptides was dynamic. The two-dimensional ^{1}H ROESY spectra of the complex of the two pentapeptides did not show intermolecular ROESY peaks. Our MD simulations corroborated the NMR results and found multiple short-lived conformations of the pentapeptide complexes. We attempted to pool together the structures of the complexes according to their root-mean-square deviation values, but these structures failed to "coalesce" into significantly populated clusters. This result confirms that the system is very dynamic, and that no conformers enjoy significant energetic advantages. Figure 2 shows four snapshots of the complex between the peptides **5** and **6c**. While the backbone of **5** is essentially helical, the backbone of **6c** adopts a "horse-shoe" conformation.

To monitor the approach of side chains in the two associating peptides, the time series described in the Materials and Methods were extracted from the trajectory. The interatomic distances between an ammonium cation of Lys and an aromatic ring of Tyr or Phe, and between an ammonium cation of Lys and a carboxylic group of Asp, ranged from 2.8 to 25 Å. Using the cutoff of 8.0 Å, on average of 4.8 and 4.7 interacting side-chain pairs were found in the complexes that **5** formed with **6b** and with **6c**, respectively. One-eighth of these interactions (13%) were the result of the contact between a Lys in one peptide and the aromatic ring (Tyr or Phe) in the other. These findings show that cation$-\pi$ contacts between the two peptides are stereochemically possible. Taken together, the NMR results and MD simulations indicate that cation$-\pi$ interactions can contribute to the association of the two pentapeptides.

Design and Structure of the Cyclic Peptide That Favors Cation$-\pi$ Interaction. The dynamic character of the pentapeptide association precludes direct observation of cation$-\pi$ interactions in these systems. Indeed, intermolecular NOEs between Lys and Tyr or between Lys and Phe were not observed. To restrain the conformational mobility of the pentapeptide complexes, we created a cyclic peptide by covalently linking the two pentapeptides. This covalent construct is better defined than the noncovalent complexes, and it allows thorough studies by two-dimensional NMR spectroscopy. In the cyclic peptides, we can spectroscopically identify cation$-\pi$ interactions.

I. Molecular-Dynamics Simulations Guided the Design of the Peptides with Cation$-\pi$ Interactions. Making minimal modifications to the primary structure of the two parent peptides, we linked them by a backbone Gly at the one end and by a disulfide bridge at the other. The product was the cyclic peptide, designated C_X. Although its conformations are more stable than those of the pentapeptide complexes, C_X is still a relatively dynamic system. Its side chains are not forced to interact; their interactions will be observed only if they stabilize the peptide conformation.

We used the results of MD simulations of the pentapeptide association to search for the best templates for the design of a cyclic peptide likely to exhibit cation$-\pi$ interactions. The simple geometric criteria stated in the Materials and Methods section proved useful in selecting suitable complexes of the two pentapeptides as template structures. A total of five such

(67) Mezei, M.; Beveridge, D. L. *Ann. N.Y. Acad. Sci.* **1986**, *482*, 1$-$23.
(68) Cubero, E.; Luque, F. J.; Orozco, M. *Proc. Acad. Sci. U.S.A.* **1998**, *95*, 5976$-$80.
(69) MacKerell, A. D., Jr. *Methods Enzymol.* **1991**, *202*, 449$-$70.

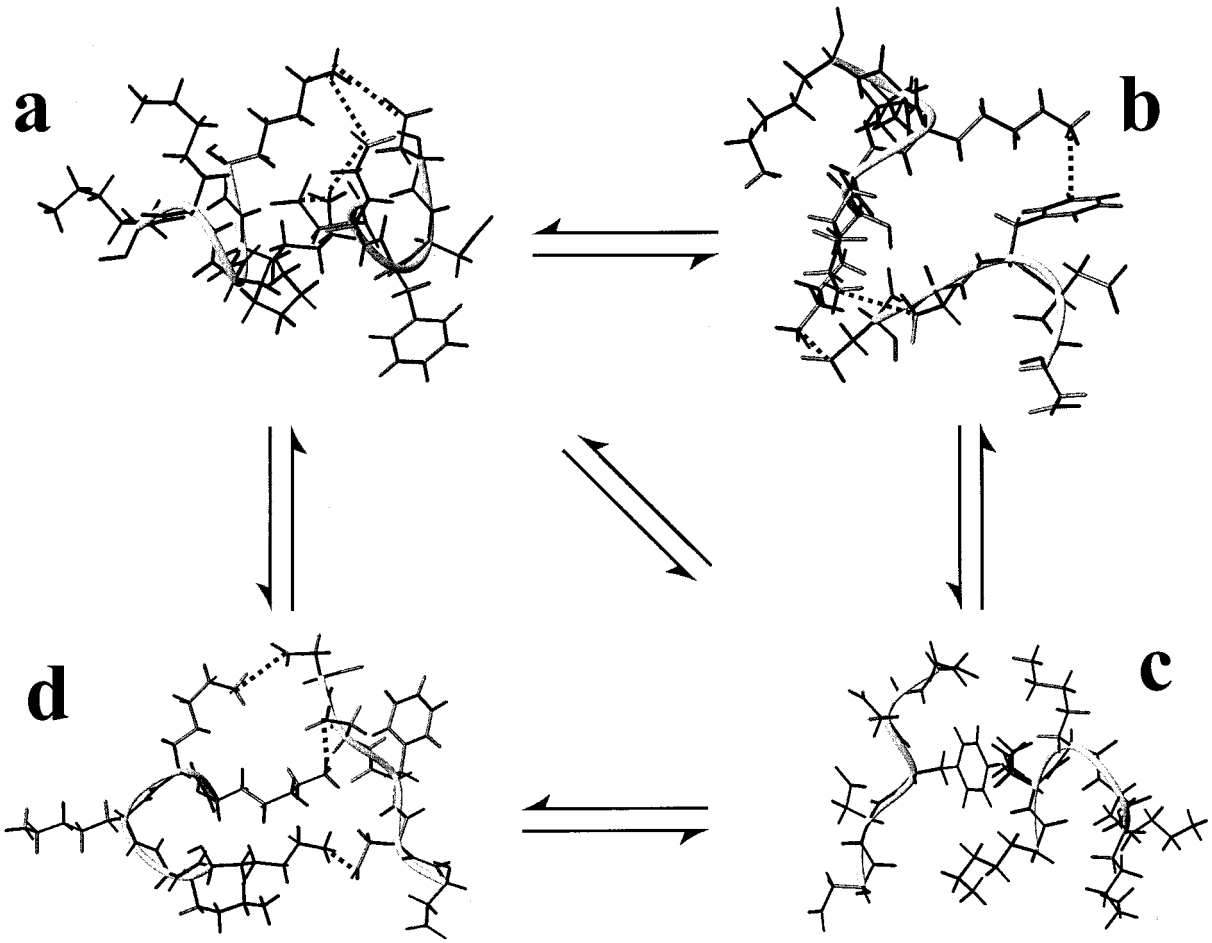

Figure 2. Families of dynamic complexes formed by the pentapeptides $AcLysLysLysLysLysNH_2$ (**5**) and $AcAspAspPheAspAspNH_2$ (**6c**). The four complexes shown represent different association modes, which have (a) four salt bridges, involving three side chains, (b) two salt bridges and one cation−π interaction, (c) no side-chain contacts, and (d) three salt bridges. The two backbones are highlighted with ribbons, and interactions are represented with dotted lines. The figure was prepared with MolMol v2K.1.[48]

templates were extracted, and their coordinates were used as starting points for the refinement of a cyclic peptide. Not all ionic side-chain contacts had to be replaced by a trial disulfide bridge. It quickly became clear that nonsymmetric replacements (i.e. of Lys2 with Cys2 and of Asp8 with Cys8) would distort the backbone structure in such a way as to prohibit the desired cation−π interaction. Replacement of ionic residues positioned within three amino acids of Gly likewise resulted in a highly strained cyclic peptide. Adding a Gly-Gly linker also proved to be unsuccessful, because the cyclic peptides became very flexible, and the cation−π interactions quickly broke.

The following three peptides were analyzed further: $AcCys(Lys)_4Gly(Asp)_2XAspCysNH_2$, $AcCys(Lys)_4Gly(Asp)_2XCysAspNH_2$, and $AcLysCys(Lys)_3Gly(Asp)_2XCysAspNH_2$. In them X was an aromatic residue. Their backbone conformations were sufficiently rigid to allow at least one Lys side chain to stay within 8.0 Å of the aromatic ring of Phe (as residue X) for 12.8, 8.6, and 16.2 ps, in the three respective peptides. For the last peptide, a similar simulation with Tyr as X was also run, with the starting coordinates as in the simulation with Phe as X. The lifetime of the cation−π interaction in this peptide was 14.3 ps, again relatively long.

The sequence $AcLysCys(Lys)_3Gly(Asp)_2XCysAspNH_2$ was chosen for synthesis and further experimental studies for two reasons. First, the simulated lifetime of the cation−π interaction was the longest in this peptide. Second, the backbone structure during the 14.3- and 16.2-ps simulations varied little (the root-mean-square deviation was less than 2.0 Å), an indication that the initial constraints were not mechanically straining the structure. Figure 3 shows the initial template structure, based on the complex of the pentapeptides **5** and **6c**, and the energy-minimized structure of the designed cyclic peptide, C_{Phe}.

II. Assignments of NMR Resonances and Structure of the Cyclic Peptide. For three reasons, we chose DMSO-d_6 as a solvent for the structure-determination experiments. First, for small peptides the populations of the folded conformations can be small, and spectroscopic measurements are strongly influenced by the populations of unstructured species. DMSO tends to destabilize all except the highly preferred conformations of the peptide, by strong polar interactions within the peptide.[70] Second, DMSO is a very viscous liquid. The extended correlation times give rise to NOESY cross-peaks that would otherwise be undetectable in aqueous solution at room temperature.[71] Third, in DMSO solution the ^1H signal of the ammonium group in lysine can be monitored, to analyze possible interactions between this group and the aromatic ring of Tyr and Phe. As Table 1 and Figure 1 show, the energies of this interaction are similar in aqueous and DMSO solutions.

Many peptides have already been studied in organic solvents.[71] Stable structures of cyclic and linear peptides identified by NMR in DMSO solution agree well with their structures

(70) Jackson, M.; Mantsch, H. M. *Biochim. Biophys. Acta* **1991**, *1078*, 231−5.

(71) Evans, J. N. S. *Biomolecular NMR Spectroscopy*; Oxford University Press Inc.: New York, 1995.

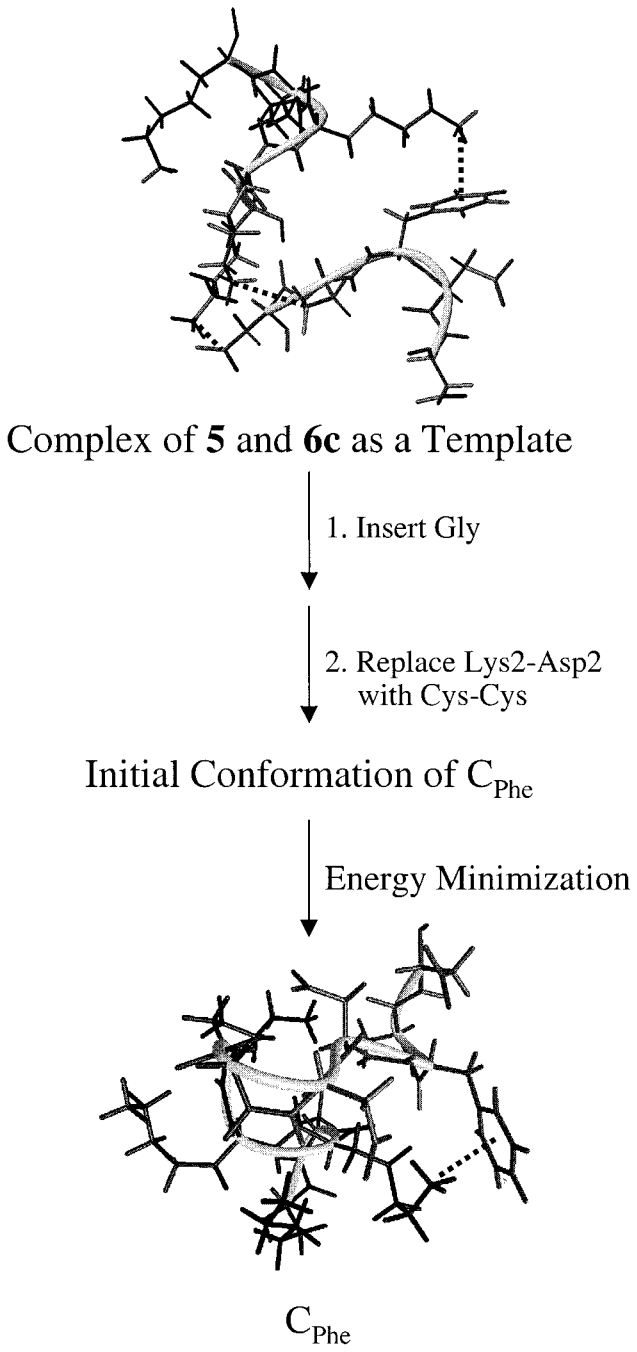

Figure 3. Design of the cyclic peptide containing cation−π interactions. The complex of the two pentapeptides was used as a structural template for a cyclic peptide. The template shown is based on the complex of pentapeptides AcLysLysLysLysLysNH$_2$ (**5**) and AcAspAspPheAspAspNH$_2$ (**6c**) with a cation−π interaction between Lys3 in **5** and the aromatic ring of Phe3 in **6c**. Connections of the two pentapeptide strands with a Gly residue and replacement of a salt bridge with a pair of disulfide-bonded cysteines yielded the starting conformation of the cyclic 11-residue peptide. Shown is its energy-minimized structure. The figure was prepared with MolMol v2K.1.[48]

determined by X-ray diffraction in crystals.[72,73] Moreover, recent studies have shown that some proteins have similar structures and functions in DMSO and in aqueous solution.[74] We will show below that the structures of our cyclic peptides, too, are very similar in DMSO and aqueous solution.

Figure 4 shows the NOESY spectrum of the cyclic peptide C_{Tyr} at 45 °C in DMSO. The dispersion of the chemical shifts and numerous NOE cross-peaks indicate that the molecule adopts a well-defined structure in solution. The NOESY spectrum of the peptide C_{Phe} is very similar (see Figure S5 in the Supporting Information).

Inspection of the amide-to-aliphatic region of the spectra reveals more than 11 different NH frequencies for this 11-residue peptide (see Figure 5). Because the peptide samples are chromatographically pure, this finding suggests that at least two conformations of the peptide are simultaneously present in solution and that they interconvert slowly on the NMR time-scale. The sequence-specific assignments of the resonances were made in the standard manner;[75] amino acid spin systems were identified primarily from the TOCSY cross-peak patterns. The sequential assignments of NMR peaks for C_{Tyr} and C_{Phe} are listed in Tables S2 and S3 in the Supporting Information, respectively. We find two sets of the chemical shifts for each of the three residues Lys3, Tyr9/Phe9, and Cys10. The two different sets of peaks corresponding to the same residue in the sequence are labeled with a residue number and this number primed, i.e., 3 and 3′, 9 and 9′, and 10 and 10′ (see Figure 5). Although we see only two sets of peaks, it is possible that a given peptide exists in more than two conformations. This multiplying of peaks arises from different microenvironments that a given residue feels in different conformations of the peptide. Later we will refer to different forms of the residue 3 as apparent "residues" 3 and 3′, likewise for residues 9 and 10.

Among the numerous NOEs there are some connecting residues that are not adjacent in the sequence. This is evidence for a well-defined and fairly rigid conformation of the peptide in solution. In the amide−amide region of the NOESY spectra, strong NH i to i+1 connections are found for residues from 3 to 5, and from 8 to 9. In addition, NH i to i+2 connections have been identified for residues 2 and 9′, and a weak NOE cross-peak from Lys4(NH) to Tyr9′/Phe9′(NH) has been observed. In the amide (NH) to α ($C^{\alpha}H$) fingerprint region of the NOESY spectra, there are strong $C^{\alpha}H(i)$−NH(i+1) NOEs for almost the entire sequence, and also additional NOEs from Gly6($C^{\alpha}H$) to Asp8(NH) and from Lys3′(NH) to Lys4($C^{\alpha}H$). In the α−α region of the spectra, there are NOEs between the $C^{\alpha}H$ protons of residues 5 and 7 and residues 3 and 8, consistent with a turn in the peptide backbone. Also there are NOEs involving α-protons of residues 2 and 3, 7 and 8, and 7 and 9. The aforementioned NOESY data indicate that the peptide has a turn centered at Gly6, that its structure is relatively tight, and that some of the side chains may interact with each other. Residues 3 or 3′, 8, and 9 or 9′ are most likely to interact with neighboring residues (including those on the opposite strand), since the backbone near the listed residues seems to be different from the rest of the peptide backbone.

Additional NMR evidence for the interactions between residues comes from the analysis of the aliphatic regions in the NOESY spectra. The NOE cross-peaks between the side-chain protons in Lys5 and $C^{\beta}H$ in Asp8 are consistent with a salt bridge between these residues. We find NOEs between the aromatic protons in residue 9 and $C^{\gamma}H$ and $C^{\delta}H$ protons in Lys3′ (see Figure 6). The intensity of these cross-peaks decreases from $C^{\delta}H$ to $C^{\gamma}H$. The cross-peak between the aromatic protons in residue 9 and $C^{\epsilon}H$ in Lys3′ is undetectable, because the

(72) Ni, F.; Ripoll, D. R.; Purisima, E. O. *Biochemistry* **1992**, *31*, 2545−54.
(73) Kessler, H.; Bats, J. W.; Griesinger, C.; Koll, S.; Will, M.; Wagner, K. *J. Am. Chem. Soc.* **1988**, *110*, 1033−49.
(74) Sivakolundu, S. G.; Mabrouk, P. A. *J. Am. Chem. Soc.* **2000**, *122*, 1513-21.
(75) Wüthrich, K. *NMR of Proteins and Nucleic Acids*; John Wiley and Sons: New York, 1986.

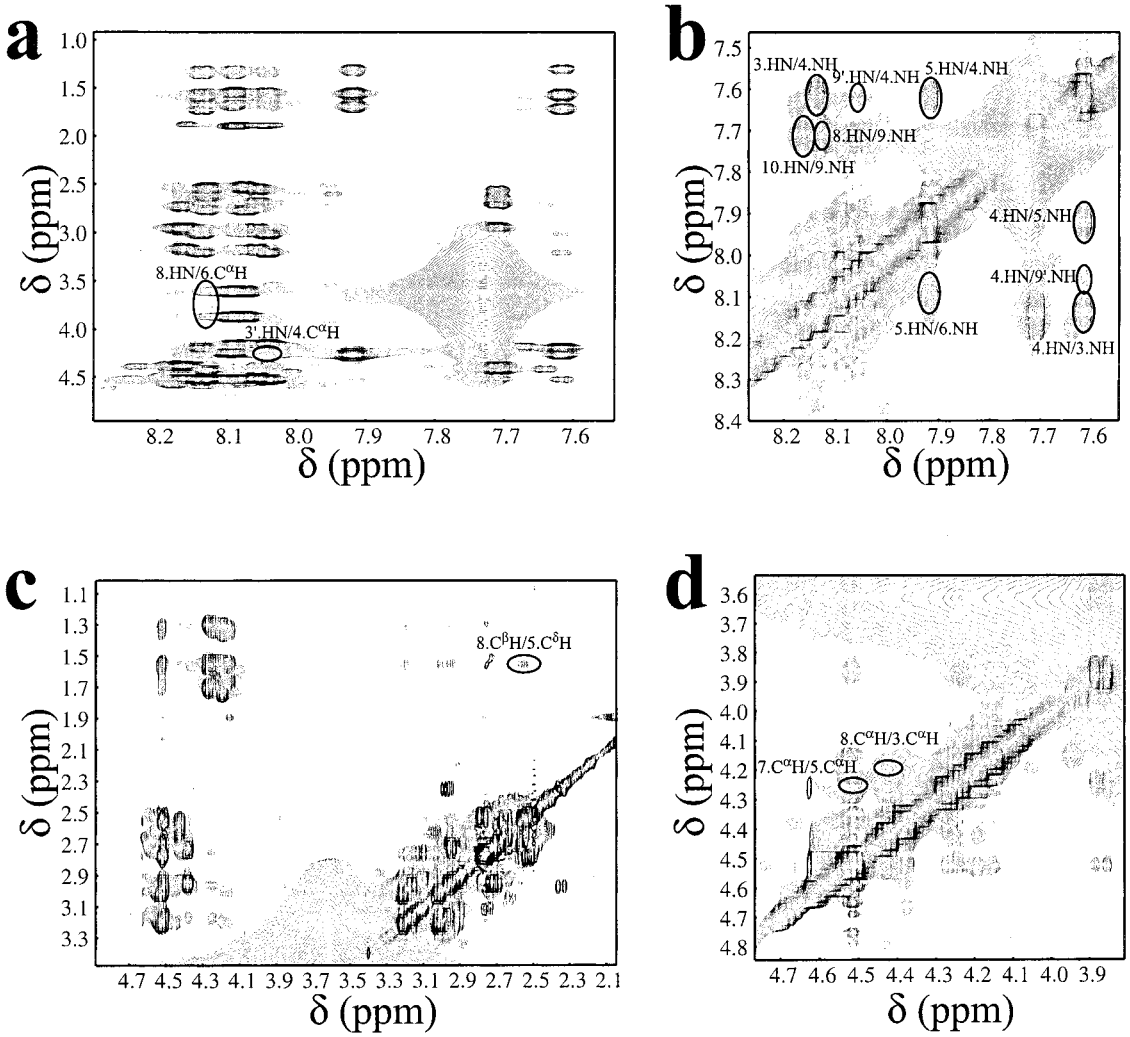

Figure 4. Selected regions of the 2D ^{1}H NOESY spectrum of the cyclic peptide C_{Tyr} dissolved in DMSO-d_6 at 45 °C: (a) amide-to-aliphatic, (b) amide-to-amide, (c) aliphatic-to-aliphatic, and (d) α-to-α. Some of the crucial cross-peaks discussed in the text are circled.

chemical shifts of C$^{\beta 2}$H in Tyr9/Phe9 and C$^{\epsilon}$H in Lys3′ happen to be the same. Furthermore, there are NOEs between C$^{\beta}$H, C$^{\gamma}$H, and C$^{\delta}$H in Lys3′ and C$^{\beta 1}$H in residue 9.

The observed cross-peaks between the aromatic and C$^{\beta}$H protons in residue 9 on the one side and aliphatic protons in Lys3′ on the other arise from direct NOE transfer, and are not a consequence of spin-diffusion. In ROESY spectra direct and singly-relayed NOE cross-peaks can be distinguished on the basis of their sign relative to the diagonal.[76] In the ROESY spectrum of C_{Tyr}, the above-mentioned cross-peaks are negative relative to the diagonal, evidence that the cross-peaks arise from direct NOE transfer. In the NOESY spectrum acquired with a shorter mixing time (100 ms), relayed transfer should become much attenuated. As expected for a molecule of this size, all NOEs became weaker when the short mixing time was used. In this experiment, the cross-peaks correlating the side chains of Lys3′ and Tyr9 were still observed, providing further evidence that these cross-peaks arise from direct NOE transfer.

The many NOEs between the side chains of residues 3′ and 9 are evidence for their close proximity. Since C_{Tyr} and C_{Phe} show similar NOE patterns, the proximity of these two side chains cannot be merely due to a hydrogen bond involving the hydroxyl group in Tyr9. Rather, we propose that a cation−π interaction is formed between the ammonium group of Lys3′

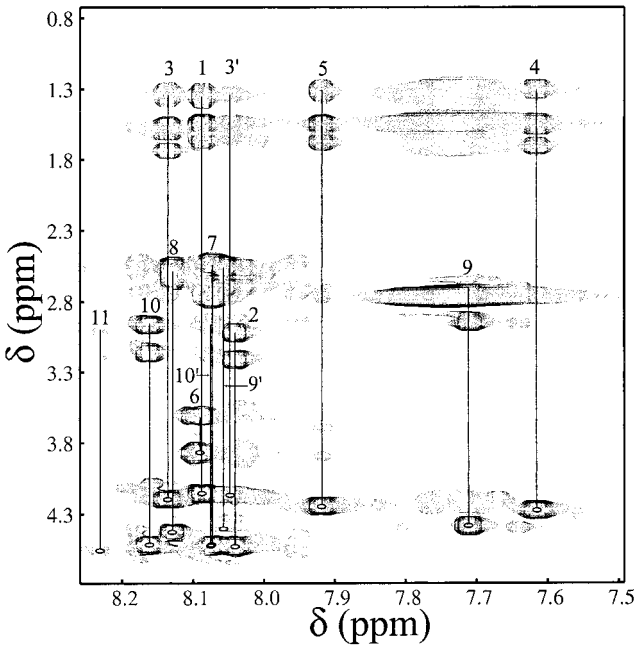

Figure 5. Amide-to-aliphatic region of the 2D ^{1}H TOCSY spectrum of the peptide C_{Tyr} dissolved in DMSO-d_6 at 45 °C. Each intraresidue spin system is marked by a solid line and labeled by the position of the amino acid residue in the peptide sequence.

(76) Bax, A.; Sklenar, V.; Summers, M. F. *J. Magn. Reson.* **1986**, *70*, 327−333.

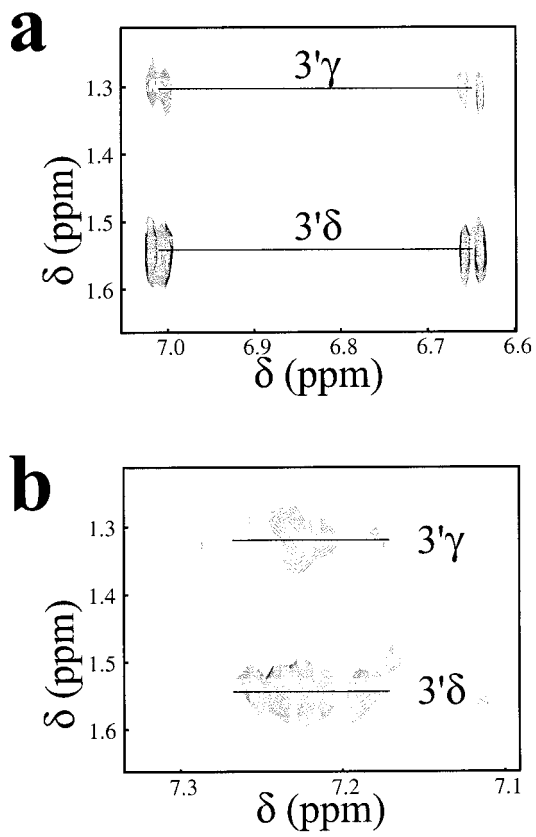

Figure 6. Portions of the 2D ^{1}H NOESY spectra of the cyclic peptides (a) C_{Tyr} and (b) C_{Phe} dissolved in DMSO-d_6 at 45 °C, showing the cross-peaks between the $C^{\delta}H$ and $C^{\gamma}H$ protons of Lys3′ on the one side and the aromatic protons of Tyr9/Phe9 on the other.

and the aromatic ring of Tyr9/Phe9. The side chains of Lys3′ and Tyr9/Phe9 appear to be positioned inside a turn of the peptide backbone. The aromatic protons of Tyr9/Phe9 have multiple NOEs with the neighboring residues, Asp8 and Cys10. The side chain of Lys3′ has NOEs with $C^{\beta}H$ protons in Cys2 and in Cys10, residues linked by the disulfide bond. Evidently, the expected cation$-\pi$ interactions in the cyclic peptides C_{Tyr} and C_{Phe} were indeed formed. Our simple method of peptide design proved successful.

Since there are NOEs between residues 9′ and 10′, these residues likely belong to the same peptide conformation. We did not, however, find NOEs linking residues 3′ and 9′ or residues 3′ and 10′. The available data suggest that the multiple conformations of the cyclic peptides C_{Tyr} and C_{Phe} can be divided into three distinct families: C_X*, which contains residues 3, 9, and 10; $C_X^{3'}$, which contains residues 3′, 9, and 10; and $C_X^{9'10'}$, which contains residues 3, 9′, and 10′.

NMR solution structures for the three families of the cyclic peptides C_{Tyr} and C_{Phe} were calculated from constraints obtained from the NOESY spectra, as described in the Materials and Methods section. Figure 7 shows the average calculated structures for the three families of the peptide C_{Tyr}, consistent with the experimental data. Such families exist also for the cyclic peptide, C_{Phe}. The three families have their own distinct features. In C_X* (Figure 7a), the side chains of four Lys, three Asp, and Tyr/Phe are extended into the solvent; there are no interactions between the residues within the molecule. In $C_X^{3'}$ (Figure 7b), the ammonium cation of Lys3 and the aromatic ring of Tyr9/Phe9 form a well-defined cation$-\pi$ interaction. The two interacting residues are situated inside the peptide; Tyr9/Phe9, Lys3, and the disulfide bridge combine to form a hydrophobic

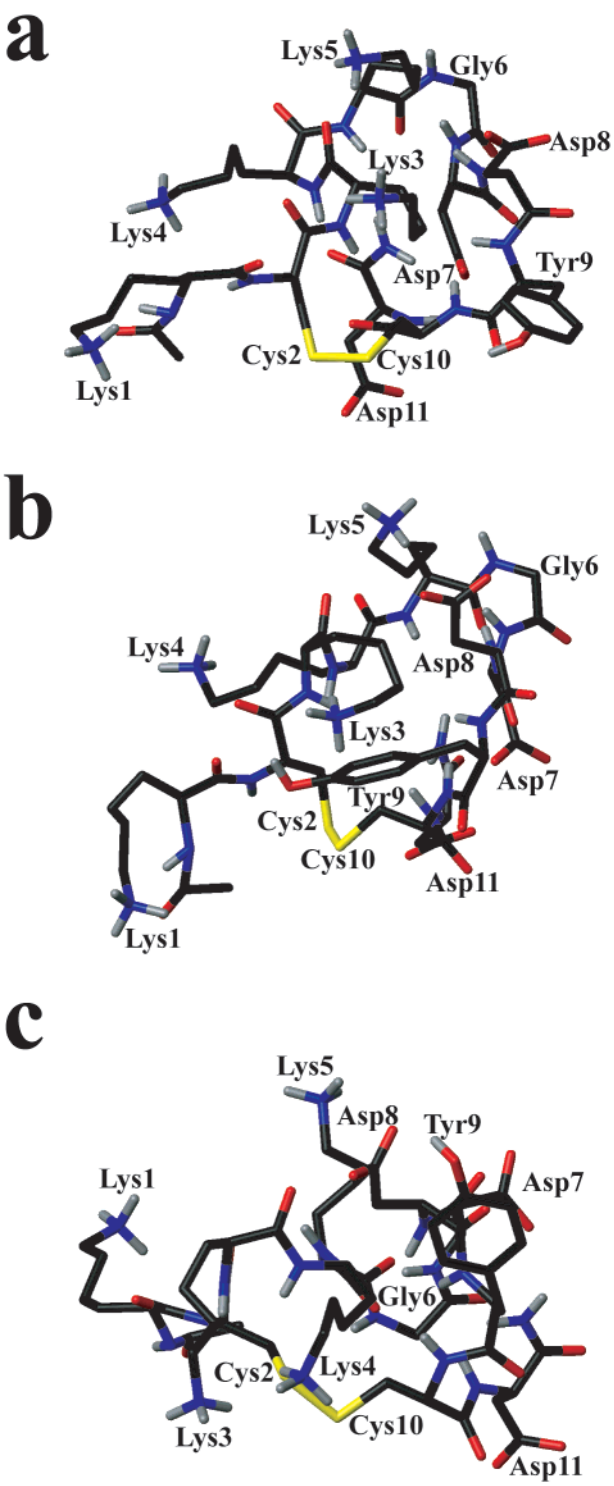

Figure 7. Calculated structures for the three families of the cyclic peptide C_{Tyr}: (a) C_{Tyr}*, (b) $C_{Tyr}^{3'}$, and (c) $C_{Tyr}^{9'10'}$. For each family, 100 structures were generated, and the average of the 10 having lowest energy is shown. Hydrogen atoms bonded to carbons are omitted, for clarity. The figure was prepared with MolMol v2K.1.[48]

core of the peptide. In $C_X^{9'10'}$ (Figure 7c), residues Lys5 and Asp8 form a salt bridge.

The root-mean-square deviation values for the backbone (C, C^{α}, O, NH) atoms for 10 lowest-energy structures in each of the three families of the peptide C_{Tyr} fall between 0.4 and 1.0 Å, and the root-mean-square deviation values for all atoms fall between 1.2 and 2.1 Å; these values are listed in Table S5 in the Supporting Information. Because peptide structures based on NOE restraints are known to be insensitive to rapid

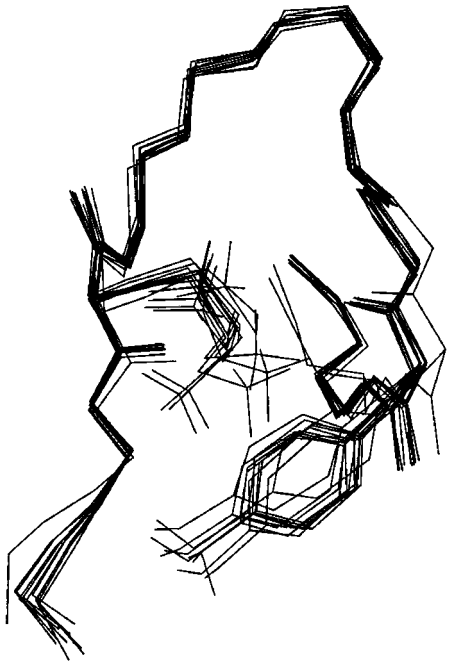

Figure 8. Ten lowest-energy structures in the family $C_{Tyr}3'$ of the cyclic peptide C_{Tyr}, showing the peptide backbone and the side chains of Lys3 and Tyr9. Their cation−π interaction is evident. Hydrogen atoms bonded to carbons are omitted, for clarity. The figure was prepared with MolMol v2K.1.[48]

conformational change and tend to be biased toward the most compact structure,[77] the root-mean-square deviation values should be viewed with caution.

Figure 8 shows the 10 lowest-energy structures for one of those families, $C_{Tyr}3'$. The peptide has a well-defined structure, with limited flexibility. As expected, the central region of the peptide is rigid, whereas the terminal regions are more flexible.

III. Cation−π Interactions between Amino Acid Side Chains in the Cyclic Peptides. The designed cyclic peptides C_{Tyr} and C_{Phe} adopt multiple conformations in solution. From two-dimensional NMR data we deduced three different structures, corresponding to three distinct families of peptide conformations. In the family C_X3', the side chain of Lys3 lies close to the aromatic ring of residue 9, as evidenced by many medium-range and long-range NOEs, discussed above. We attribute this proximity to a cation−π interaction between the two side chains. The two residues remain close even at higher temperatures; the same NOEs between the protons in Lys3′ and protons in Tyr9/Phe9 persist at 60 °C.

Analysis of the chemical shifts provides further evidence for the cation−π interaction between Lys3′ and Tyr9/Phe9. Because ^{1}H NMR signal of the $N^\epsilon H_3^+$ group of lysines is broad, the $N^\epsilon H$ protons of all lysines appear to have the same chemical shift and therefore are unsuitable for monitoring the specific interaction with the aromatic residue. However, the signals of the $C^\epsilon H$ and $C^\delta H$ protons in Lys3′ occur at approximately 0.03 and 0.02 ppm, respectively, upfield from the signals of the $C^\epsilon H$ and $C^\delta H$ protons in other lysines (see Tables S2 and S3 in the Supporting Information). The upfield positions of the above-mentioned signals are consistent with placement of the side chain of Lys3′ above an aromatic ring, a consequence of the cation−π interaction between Lys3′ and Tyr9/Phe9.

Figure 8 shows 10 lowest-energy structures for the family $C_{Tyr}3'$ of the cyclic peptide C_{Tyr} and the interactions between the side chains of Lys3 and Tyr9. The cation−π interactions between these side chains are well-defined for most of the structures. Figure S6 in the Supporting Information shows this interaction in detail. The distances between the N^ϵ atom in Lys3 and the aromatic carbon atoms in Tyr9 range from 2.5 to 4.6 Å; these values are quite reasonable in view of those reported for cation−π interactions between amino acid side chains in protein structures.[7] As a test, we additionally constrained the distance from the ammonium group in Lys3 to the carbon atoms in the aromatic ring of Tyr9 in calculations of the $C_{Tyr}3'$ structure. With these constraints set at ≤4.0 Å,[7] the all-atom root-mean-square deviation values for the 10 lowest-energy structures decreased from 1.2 to 1.1 Å (see Table S5 in the Supporting Information). In the average structure obtained with these additional constraints, the ammonium cation of Lys3 sat more symmetrically over the aromatic ring, with the distances between the N^ϵ atom in Lys3 and the aromatic carbon atoms in Tyr9 ranging from 2.8 to 4.1 Å. We, however, chose to present here the structure based on the experimental (NOE) data alone, with no artificial constraints added.

Cation−π Interaction Compacts the Structure of the Cyclic Peptide. Our structural evidence shows that the residues 3 and 9 are tightly packed inside the peptide turn. In principle, other interactions, besides the cation−π interaction, can contribute to the proximity of the two side chains. The aliphatic portion of the Lys side chain may have hydrophobic contacts with the aromatic ring of Tyr or Phe and with the disulfide bridge. The ammonium group of Lys can also form a salt bridge with a side chain of one of the nearby aspartates or a hydrogen bond with other peptide groups. We investigate the possibility of these additional interactions in the discussion that follows.

If the close contact between the residues 3 and 9 is mainly due to hydrophobic and/or hydrogen-bonding interactions involving Lys3, then replacement of aromatic residue 9 with an aliphatic amino acid of similar size should keep the side chains of residues 3 and 9 in the proximity to each other. Our experiments, however, showed that replacement of the aromatic residue in position 9 with leucine (in the cyclic peptide C_{Leu}) abolishes the contact between the side chains of Lys3 and residue 9. In the NMR spectra of C_{Leu} we find no NOEs diagnostic of the proximity of these side chains. The hydrophobic Leu residue is packed inside the peptide, as indicated by the NOE cross-peaks from the $C^\delta H$ protons in Leu9 to the NH and $C^\alpha H$ protons in Asp8 and to the NH proton in Cys10. The lack of NOEs for the side chain of Lys3 suggests that this residue is mobile and disordered, as expected for a residue exposed to the solvent. We conclude that in peptides C_{Tyr} and C_{Phe} it is the cation−π interaction between Lys and aromatic amino acids, and not some other interactions, that brings together these residues on the neighboring strands and promotes a more compact structure of the cyclic peptide.

Our two-dimensional NMR experiments, discussed so far, were done in DMSO. As mentioned above, this solvent facilitates direct observation of the cation−π ineractions in peptides. Because, however, these interactions are especially important in biological systems, we verified that we can detect them also in aqueous solution. The 2D ^{1}H NOESY spectrum of C_{Phe} in a sodium acetate buffer at pH 3.8 and 5 °C is almost identical to the spectrum in DMSO at 45 °C (see Figure S7 in the Supporting Information). We reasonably conclude that the peptide adopts similar conformations in the two solvents. In aqueous solution, as in DMSO, we detect multiple conformations of the cyclic peptide. As in DMSO, we observe the cross-peaks between the aromatic protons in residue 9 and the $C^\beta H$,

(77) Williamson, M. P.; Waltho, J. P. *Chem. Soc. Rev.* **1992**, 227−236.

$C^{\gamma}H$, and $C^{\delta}H$ protons in Lys3′, evidence for the cation−π interaction between these residues.

In the designed cyclic peptides, residue Gly and the disulfide bridge formed by Cys2 and Cys10 tightly link the neighboring strands. The cyclization promotes conformational stability of the peptides in solution and allows the detection of the cation−π interaction. We also investigated whether removal of one of the linkers would significantly alter the peptide conformation and abolish the interaction between the cationic side chain of lysine and the aromatic side chain.

Reduction of the disulfide bond in the cyclic peptide C_{Phe} by dithiothreitol yielded the acyclic product, designated AC_{Phe}. The NOESY spectrum of AC_{Phe} in a sodium acetate buffer at pH 7.6 at 5 °C shows NOEs from Asp7(NH) to Lys4($C^{\beta}H$) and Lys5($C^{\alpha}H$) and from Lys5($C^{\alpha}H$) to Gly6($C^{\alpha}H$), evidence that the acyclic peptide also adopts a turn structure. Overall, the acyclic peptide AC_{Phe} shows fewer NOEs than its cyclic counterpart, C_{Phe}, evidence that the former peptide is more flexible. Interconversions among the multiple conformations of AC_{Phe} are fast on the NMR time-scale, and only 11 NH frequencies are observed in the 2D NOESY spectra of this 11-residue peptide. Interestingly, residues Lys3 and Phe9 of the peptide AC_{Phe} still form a cation−π interaction: the cross-peaks persist between the aromatic protons in Phe9 and the $C^{\beta}H$, $C^{\gamma}H$, and $C^{\delta}H$ protons in Lys3 (see Figure 9a). Figure 9b shows 10 lowest-energy structures and the average structure of the peptide AC_{Phe}, which is less defined than the structure of C_{Phe}, because of the higher flexibility of the former peptide and fewer NOE constraints available. To conclude, the residues Lys3 and Phe9, located away from the Gly turn, interact even in the acyclic peptide, not constrained by the disulfide bridge.

The persistence of the cation−π interaction even in a more flexible peptide emphasizes the importance of these interactions for both intramolecular and intermolecular recognition, e.g. within proteins and at the protein−protein interface. Previous studies indicated that cation−π interactions may be important in stabilizing peptide and protein structures.[6,58,78,79] Our results with C_{Leu} and AC_{Phe} demonstrate that cation−π interactions between side chains help in forming more compact peptide structures.

Perturbations of pK_a Values as a Criterion of Cation−π Interactions in the Dynamic Systems. The NOE cross-peaks and analysis of chemical shifts consistently showed the existence of cation−π interactions in the cyclic peptides C_{Tyr} and C_{Phe}. Another criterion for cation−π interactions, used mostly in studies of proteins, is perturbation of the pK_a values of the interacting side chains. Cation−π interaction may be expected to raise the pK_a of the cationic side chain, because it becomes additionally stabilized by the aromatic ring.[2,58] Peptides, unlike proteins, are flexible. The same set of residues may have different interactions in various conformations of a peptide. In principle, the observable (macroscopic) pK_a value of a titratable residue will be a composite of the unobservable (microscopic) pK_a values of that residue in different conformations.

To check if the interaction with the aromatic ring would noticeably alter the pK_a values of the Lys residue involved, we determined these values for all four Lys residues in each of the three cyclic peptides C_X, in which X is Leu, Tyr, and Phe. The chemical shifts of nuclei proximate to the titratable group are sensitive to its protonation state.[80] To obtain individual titration curves ($C^{\epsilon}H$ chemical shift vs pH) for each of the four lysines in three peptides C_X (total of 12), we did a two-dimensional ^{1}H TOCSY experiment for each point in those curves.

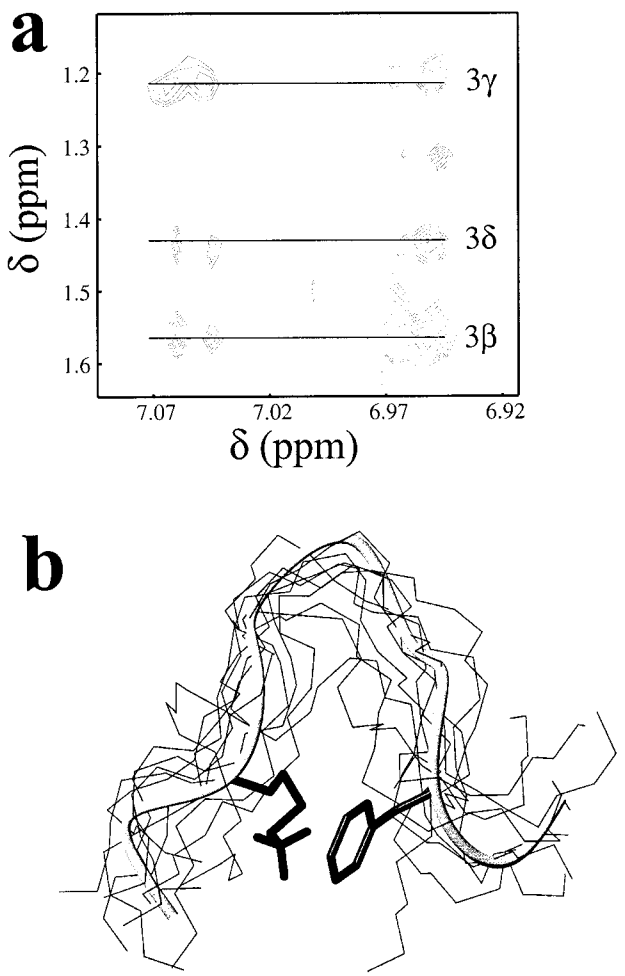

Figure 9. (a) A portion of the 2D ^{1}H NOESY spectrum of the acyclic peptide AC_{Phe} in a sodium acetate buffer at pH 7.6 and 5 °C, showing the cross-peaks between the aliphatic protons in Lys3 and the aromatic protons in Phe9. (b) Ten lowest-energy structures of the acyclic peptide AC_{Phe}. The peptide backbone is drawn for all 10 structures. The backbone of the average structure is represented by the thick ribbon. The side chains of Lys3 and Tyr9 in the average structure are shown in the stick mode. Hydrogen atoms bonded to carbons are omitted, for clarity. The figure was prepared with MolMol v2K.1.[48]

Table 3. Residue-Specific Acid Dissociation Constants (K_a)[a,b] of Lysine Side Chains for Cyclic Peptides C_X at 25 °C

	pK_a			
peptide	Lys1	Lys3	Lys4	Lys5
C_{Leu}	10.60 ± 0.07	10.58 ± 0.08	10.56 ± 0.12	10.60 ± 0.07
C_{Tyr}	10.65 ± 0.09	10.74 ± 0.07	10.57 ± 0.07	10.57 ± 0.10
C_{Phe}	10.56 ± 0.07	10.77 ± 0.07	10.69 ± 0.06	10.58 ± 0.06

[a] The pK_a values were obtained from the fittings of pH dependence for the chemical shifts of the lysine $C^{\epsilon}H$ protons, determined from the 2D ^{1}H TOCSY spectra of C_X. [b] The error margins include two standard deviations and correspond to the confidence limit greater than 95%.

The residue-specific pK_a values were determined from fittings of each of the 12 titration curves to eq 3. The results are presented in Table 3, and two of the curves are shown in Figure 10. As Table 3 shows, the pK_a values of all four lysines in C_{Leu} are the same. Evidently, their microenvironments in C_{Leu} are very similar. Since these pK_a values are identical to that of an isolated Lys group (pK_a = 10.53, reported without error

(78) Rico, M.; Santoro, J.; Bermejo, F. J.; Herranz, J.; Nieto, J. L.; Gallego, J.; Jimenez, M. A. *Biopolymers* **1986**, *25*, 1031−1053.
(79) Shoemaker, K. R.; Fairman, R.; Schultz, D. A.; Robertson, A. D.; York, E. J.; Stewart, J. M.; Baldwin, R. L. *Biopolymers* **1990**, *29*, 1−11.
(80) Rabenstein, D. L.; Sayer, T. L. *Anal. Chem.* **1976**, *48*, 1141−1146.

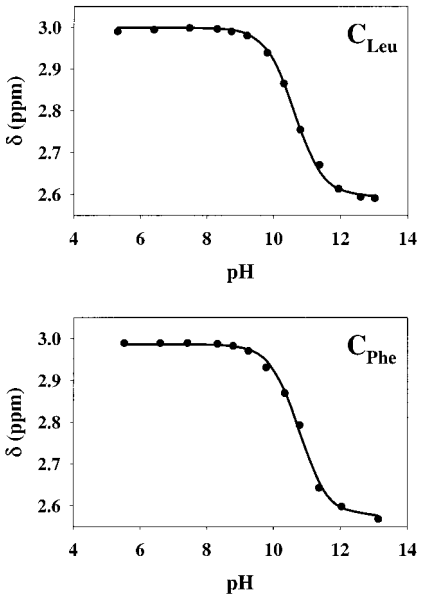

Figure 10. Titration curves for the C$^{\epsilon}$H protons in Lys3 of the cyclic peptides C_{Leu} and C_{Phe}. The former peptide lacks, while the latter one has, aromatic residue in position 9, available for cation−π interaction with Lys3. The solid lines are fits to eq 3. The pK_a values are listed in Table 3.

margins),[81,82] it is reasonable to conclude that the side chains of these four residues are exposed to the solvent and fully hydrated. These results are consistent with our NOE findings, discussed above.

In peptides C_{Tyr} and C_{Phe}, the pK_a values of Lys3 are marginally higher, while the pK_a values of the other three lysines are similar to those of the lysines in C_{Leu}, considering the conservative error margins of two standard deviations. Evidently, Lys3 resembles other lysine residues when cation−π interaction is impossible, in C_{Leu}, but differs from them when this interaction is possible, in C_{Tyr} and C_{Phe}. These facts support our previous conclusion, namely that the cation−π interactions occur in the last two peptides.

Although the cation−π interactions exist, the increase in the pK_a value of Lys3 is relatively small. A pK_a of 11.0 was reported for *N*, *N*-dimethyllysine interacting with Phe in the interhelix region between two antiparallel peptides.[83] It is debatable, however, whether the methylated derivative is a proper mimic, in view of its both steric and electronic properties, for the natural amino acid. It is unclear how much, if at all, the value of 11.0 is higher than the normal pK_a of *N*,*N*-dimethyllysine.

In this noninvasive study of natural amino acids in peptides, we find only a slight increase in the pK_a value of the interacting Lys residue. This result is understandable because the peptide adopts multiple conformations in solution, and not all of them contain the cation−π interaction.

Although pK_a values of side chains reflect cation−π (as well as other) interactions, analysis of these values is an indirect and ambiguous criterion. Analysis of chemical shifts, and especially NOEs, is a more reliable method for identifying and studying cation−π interactions in dynamic systems.

(81) Dawson, R. M. C., Ed. *Data for Biochemical Research*; Clarendon Press: Oxford, 1959.

(82) Smith, E. L. *Principles of Biochemistry, General Aspects*; McGraw-Hill: New York, 1983.

(83) Lund-Katz, S.; Phillips, M. C.; Mishra, V. K.; Segrest, J. P.; Anantharamaiah, G. M. *Biochemistry* **1995**, *34*, 9219−26.

Conclusions

Our experimental $\Delta G°$ values for cation−π interactions between amino acid side chains suggest that these interactions can be as strong as the familiar salt bridges and hydrogen bonds. By analyzing the dynamic association of the two pentapeptides, we find that various interactions work in concert. Preorientation of the cationic and aromatic side chains by multiple forces appears to be crucial for producing a stable cation−π interaction. With molecular-dynamics simulations, we designed peptide systems that showed prominent cation−π interactions between amino acid side chains. In the designed peptides, both cyclic and acyclic, cation−π interactions were clearly evident from both chemical shifts and NOEs. With model systems, such as those presented here, one can address questions of protein structure and protein−protein interactions that are difficult to address with proteins themselves. Our relatively simple design strategy was successful; it may prove to be useful in future studies of peptide and protein engineering.

Cation−π interactions are commonly found within proteins, which are relatively static structures. Our theoretical and experimental results show that these interactions occur also between and within peptides, which are dynamic structures. In dynamic systems, however, these elusive interactions may be detectable only by carefully chosen methods. This study of dynamic structures shows that cation−π interactions strongly contribute to biomolecular association. They should be sought in intermolecular recognition across dynamic protein−protein interfaces and in intramolecular processes such as protein folding.

Acknowledgment. This work was supported by the U.S. National Science Foundation, through Grant MCB-9808392. We thank Dr. G. Matthias Ullmann for valuable discussions, Mr. Nebojša M. Milović for help with HPLC purification, Professors Amy H. Andreotti and Nenad Juranić for useful suggestions about the manuscript, and Professor Peter A. Kollman for advice about MD simulations. E.V.P. thanks Dow Chemical Company for the 1999 and 2000 Fellowships awarded by the Department of Chemistry. A.T.L. thanks the U.S. National Science Foundation for support under IGERT training grant 9972653.

Supporting Information Available: Five tables showing the association constants, K_A, determined with two different titration protocols; proton resonance assignments of cyclic peptides C_{Tyr}, C_{Phe}, and C_{Leu}; the root-mean-square deviation values for 10 lowest-energy structures of the cyclic peptide C_{Tyr}; seven figures showing complexation-induced perturbations of the chemical shifts of protons in **3** upon addition of **1**; complexation-induced perturbations of the chemical shifts of the C$^{\delta}$H and C$^{\epsilon}$H protons in **3** upon addition of **1**; complexation-induced perturbations of the chemical shifts of protons in **6b** upon addition of **5**; portions of 2D ^{1}H ROESY spectra of the pentapeptides **6a**, **6b**, and **6c**; selected regions of the 2D ^{1}H NOESY spectrum of the cyclic peptide C_{Phe} in DMSO-d_6; details of the cation−π interaction between Lys3 and Tyr9 in the structure $C_{Tyr}{}^{3'}$; 2D ^{1}H NOESY spectrum of the cyclic peptide C_{Phe} in a sodium acetate buffer of pH 3.8 (PDF). This material is available free of charge via the Internet at http://pubs.acs.org.

JA010401U